

Dynamics of Lidar Reflections of the Kamchatka Upper Atmosphere and Its Connection with Phenomena in the Ionosphere

V. V. Bychkov and B. M. Shevtsov

*Institute of Cosmophysical Research and Radiowave Propagation, Far Eastern Branch, Russian Academy of Sciences,
ul. Mirnaya 7, Paratunka, Kamchatka krai, 684034 Russia*

e-mail: vasily@ikir.ru

Received March 1, 2011; in final form, October 9, 2011

Abstract—The results of Rayleigh lidar sounding of the upper atmosphere over Kamchatka are analyzed in comparison with ionosonde data. A correlation between light backscattering signals at a wavelength of 532 nm and parameters determining the content of plasma in the nocturnal F_2 layer of the ionosphere is found. Based on the performed analysis of lidar data and the geophysical situation, a hypothesis about the possible role of Rydberg atoms in the formation of lidar reflections at ionospheric heights is discussed.

DOI: 10.1134/S0016793212060047

1. INTRODUCTION

It is commonly accepted that lidar signals from within the range of heights above 100 km are absent during Rayleigh lidar sounding of the atmosphere. The mean signal from these heights is often used for determining the background signal. At the same time, in observations performed in Kamchatka in 2008–2009, it was found that the difference between the mean signal from the height range 200–300 km and independently measured background signals correlates on some days with the content of plasma in the region of the maximum of the nocturnal ionospheric F_2 layer. In this work, a possible physical mechanism explaining this correlation is discussed, namely, the formation of lidar reflections from ionospheric heights as a result of scattering on Rydberg atoms appearing as a result of electron eruptions.

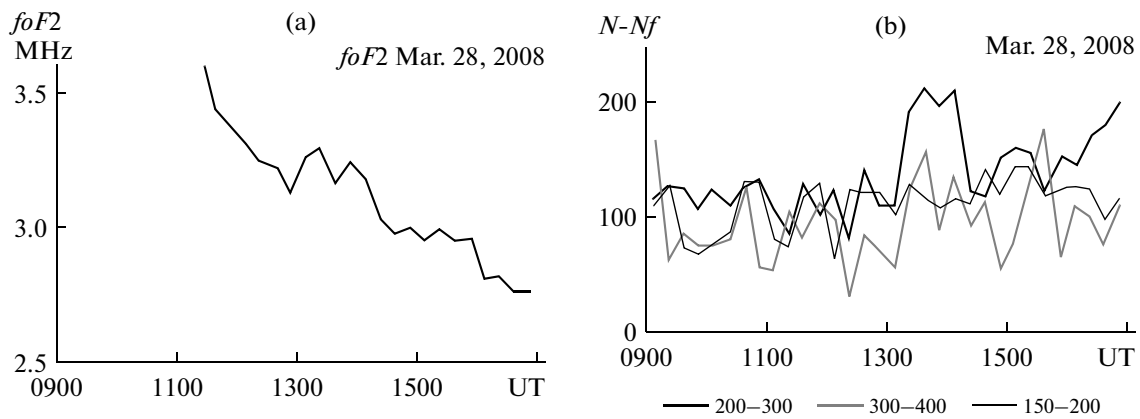
2. OBSERVATION RESULTS

A correlation between lidar signals and the state of the ionosphere was found in experimental studies of the aftereffect of a photoelectron multiplier (FEM) and the slope of total lidar signals in respect of the axis of heights; the slope was caused by the aftereffect and remained above 100 km. The frequency of the used Brilliant B laser was 10 Hz, the pulse energy was 0.4 J, and the distance between the axes of the receiver and the sender was 510 cm. In the receiving telescope, a diaphragm of 1.5 mm was used, which corresponds to the receiver's angle of vision of 7.5×10^{-4} rad. The signal was accumulated during ~ 8 h and in total contains 268400 unit echo signals. To exclude FEM illuminations from signals of the near zone, electron blocking of the FEM was used by a pulse with a duration of 140 μ s. The signal was detected during 4 ms after send-

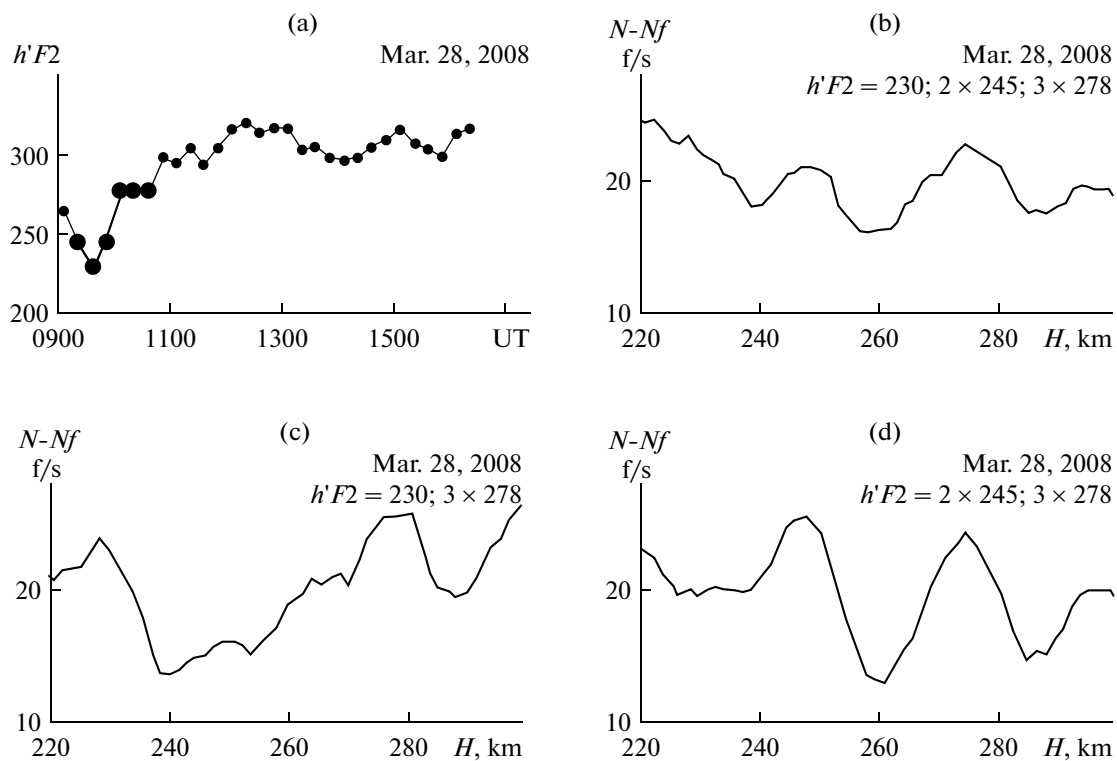
ing each light pulse of the laser with a step of 10 μ s, which corresponds to a range of heights from 21 to 600 km with a height step of 1.5 km. The value of the background signal was obtained by averaging 400 background values measured during the time interval from the 20th to the 24th milliseconds after sending each laser pulse.

The background signal of March 28, 2008, was ~ 60 – 70 photons/s during all eight hours of observations; among them, ~ 20 photons/s account for the dark noise of the FEM. Such background values are usually observed during moonless nights. A verification carried out using an astronomical calendar demonstrated that, although the lunar phase was 0.66 on that day, the moonset took place at 0725 UT; at the same time, the lidar observations began at 0900 UT. The ratio of the signal to the background value accepted values exceeding unity up to a height of 600 km. The average ratio of the signal to the background value was 1.5 over the interval 150–200 km, 1.3 over the interval 200–300 km, and 1.2 over the interval 300–400 km.

Figure 1a presents the foF_2 behavior, critical frequency of the F_2 layer on that day constructed using 15-min values measured by the Kamchatka automatic ionosphere station (AIS). In the foF_2 plot from 1300 to 1438 UT, one can observe a small, but rather sharp, increase in foF_2 . At the same time, the virtual height of the F_2 layer, $h'F_2$, decreases by more than 40 km by 1430 UT (Fig. 2a). The changes in the behavior of the height and frequency of the F_2 layer are synchronous and can be connected with the amplification of corpuscular eruptions of ionizing particles over the observation point. The presence of nocturnal sporadic E_s layers of the corpuscular type on that day according to the Kamchatka AIS verifies this hypothesis.



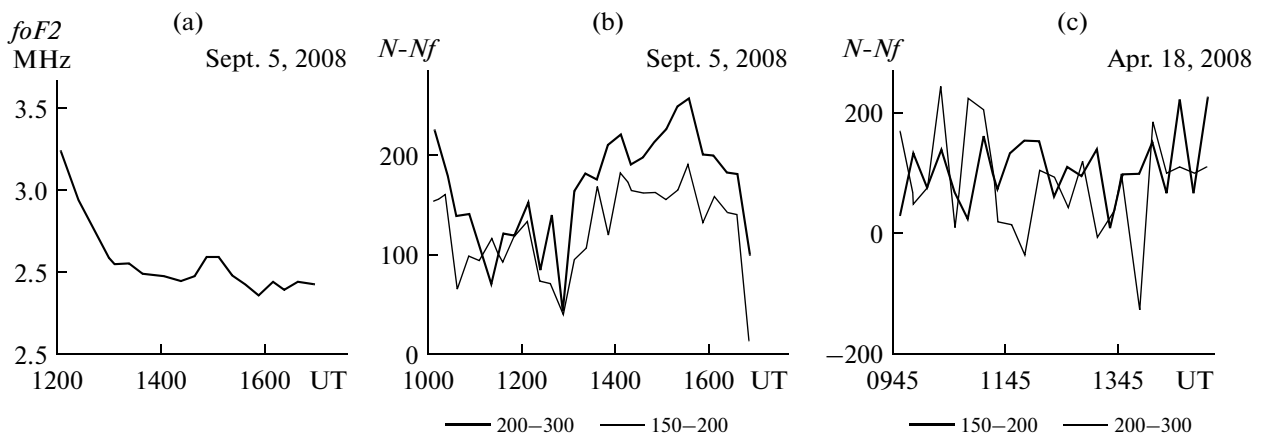
1 **Fig. 1.** (a) Behavior of the critical frequency of the $F2$ layer on March 28, 2008, and (b) total lidar signal from a height regions of 200–300, 300–400, and 150–200 km.



1 **Fig. 2.** Lidar signal summated according to the criterion of the $h'F2$ value during its accumulation.

1 Figure 1b presents the lidar “signal minus background” from the ranges 200–300, 300–400, and 150–200 km. It was obtained by summing up the corresponding quantities in 1.5-km layers. No correlation is observed between the values of the $foF2$ curve and the lidar signal from a range of 150–200 km. In the signal from a range of 200–300 km, a burst coinciding in time with the $foF2$ burst is observed. An insignificant

shift in time between the bursts on the two curves is explained by the fact that the lidar data were accumu- 1 lated during ~ 15 min whereas the séance of ionosphere sounding continued 45 s. With allowance for this fact, one can state that not only the times of the appearance of singularities in the behavior of the sig- 2 nals coincide but also the morphology of the signals: the burst in the lidar and ionosphere data has a double- 1



1 **Fig. 3.** Behavior of the (a) critical frequency of the $F2$ layer and (b) lidar signals on September 5, 2008, and (c) April 18, 2008.

peak structure. The values of the “signal minus background” plot from a range of 300–400 km retain the correlation with the behavior of ionospheric $foF2$, but the intensity of the signal decreases and its fluctuations are amplified.

1 Another type of correlation between the total lidar signals and the position of the $F2$ -layer maximum in early nocturnal hours was detected on the same day from 0900 to 1030 UT. Figure 2a presents the $h'F2$ behavior during the lidar observations. Figures 2b–2d present lidar signals averaged over 15-min samples from the interval from 0900 to 1030 UT. The samples are grouped according to the $h'F2$ values observed at the instant of lidar signal accumulation. The $h'F2$ value corresponding in time is designated on the inscription in the upper part of Figs. 2b–2d. To ensure the correctness of the comparison, the signals were normalized so that their dimension is expressed in photon per second. The lidar signals were smoothed in height by the moving average method.

1 The presented figures demonstrate a correlation between the lidar signal and $h'F2$. The local maximums in the total signal correspond to the $h'F2$ position detected by the AIS at the time of data accumulation. The elimination of 15-min lidar signals from the sample decreases the average signal in the range of heights where the $F2$ layer was present at the time of accumulation of the eliminated lidar data and vice versa. The possibility to accumulate such a signal and to detect this correlation is caused by fast variations in the height of the $F2$ layer under the conditions of retained geomagnetic perturbation and by a delay of the layer at a height of 278 km during ~45 min and in a region of 245 km during ~30 min.

1 Illustrations using other combinations of data sets are not presented, but they also verify the correlation with the position of the $F2$ -layer maximum. A study of the data of lidar and ionospheric observations for other days of 2008 revealed more cases of correlation between lidar signals and the plasma content during a

maximum of the nocturnal ionospheric $F2$ layer. We compared total “signal minus background” values from ranges of 150–200 and 200–300 km. The maximal values of the “signal minus background” difference are related to a height range of 200–300 km in all cases. A correlation between lidar signals from different regions was also observed with correlation coefficients of 0.6–0.9 and with a confidence interval of about 0.2, which must not be observed for signals from these heights and which is not observed on usual days.

For example, Fig. 3a presents data on the $foF2$ behavior and Fig. 3b shows lidar signals averaged over 1 ranges of 150–200 and 200–300 km obtained on September 5, 2008. An untypical increase in $foF2$ at the nocturnal time between 1400 and 1600 UT and an increase in the values of the lidar signals coincide in time. At the same time, a decrease in $h'F2$ from 300 km at 1400 UT to 250 km at 1500 UT, followed by a return to 300 km at 1600 UT, was observed (a picture is not presented). The coefficient of correlation between the signals from height ranges of 150–200 and 200–300 km is 0.802. The observations continued from 0945 to 1630 UT, and the data series contain 28 numbers; the confidence interval is (0.68–0.92) at a significance level of 0.10 according to Student’s test. These figures are justified in the Appendix. This example demonstrates that increased values of lidar signals can also be observed from a range of 150–200 km; it qualitatively verifies the correlation between lidar signals from ionospheric heights and the $foF2$ value.

1 Similar data with a coefficient of correlation between signals from different ranges of heights of about 0.8 and increasing $foF2$ values during an increase in lidar signals were also obtained on the next day (September 6, 2008). The pictures are similar to Fig. 3 and are not presented. The correlation coefficient for the data in Fig 3c for the usual day of April 18, 2008, is 0.02.

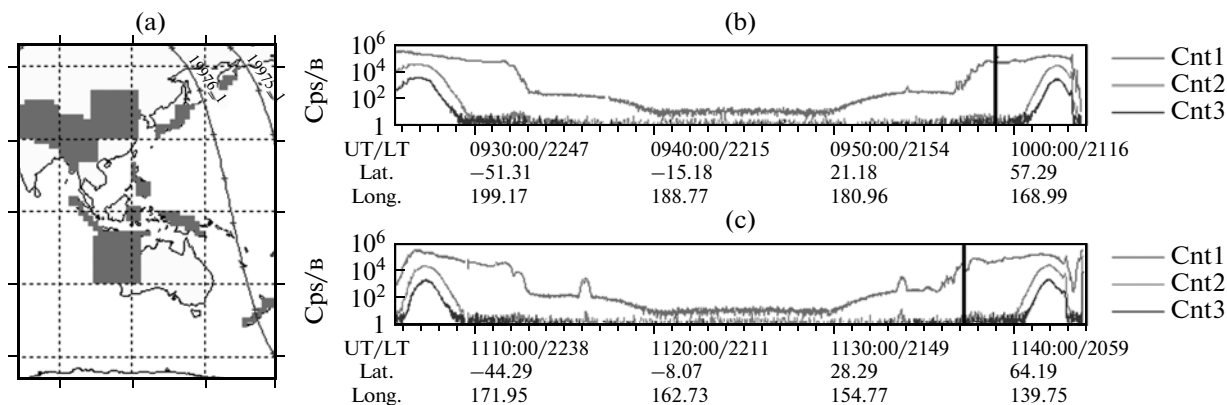


Fig. 4. (a) Trajectories of the orbits of the Demeter satellite on March 28, 2008, and (b, c) electron fluxes along these trajectories.

3. GEOPHYSICAL SITUATION

All of the correlations were detected under the conditions of geomagnetic perturbations and were accompanied by the appearance of sporadic *Es* layers of the corpuscular type. In all cases, the Demeter satellite (<http://demeter.cnrs-orleans.fr/>) flying over Kamchatka directly during nocturnal lidar observations at a height of 660 km detected an increase in relativistic electron fluxes.

The observations on March 28, 2008, were performed on the third day after the storm that took place on March 26, 2008. The average value of the *Kp* planetary index on March 28, 2008, was 3.79 (<http://spidr.ngdc.noaa.gov/spidr/index.jsp>). According to the data of the geomagnetic observatory at the Institute of Cosmophysical Research and Radiowave Propagation, the values of the *K* indices on March 28, 2008, were 2, 2, 4, 4, 3, 2, and 2. The *K* indices detected directly during the lidar observations are highlighted in bold. The values of the *K* indices on September 5, 2008, were on average typical of quiet magnetic conditions. However, on the previous day of September 4, 2008, a geomagnetic perturbation took place with the following values of the local *K* indices: 4, 4, 4, 3, 4, 4, 2, and -. The value of the planetary *Kp* index on September 4, 2008, was 5.7, 6, 3.7, 3.3, 3.7, 3.3, 2.3, and 2.3. According to the ionospheric data of September 5, 2008, pronounced sporadic *Es* layers of the corpuscular type were observed at a height of 100 km during almost the entire period of lidar observations; the *foEs* value reached 2.5–2.8 MHz.

The presence of relativistic electron eruptions during the lidar observations is verified by data from the Demeter satellite. Figure 4a presents the orbits of the Demeter satellite for March 28, 2008, to the east and to the west of Kamchatka. Figures 4b and 4c present the total number of electrons detected per second when moving along these orbits. The black vertical lines mark the instants at which the satellite crossed a latitude of 53°N, where the lidar and the Kamchatka AIS are located.

The Demeter artificial satellite measured electron fluxes at three channels: Cnt1 (90.7–526.8 keV), Cnt2 (526.8–971.8 keV), and Cnt3 (971.8–2342.4 keV). At the orbit that passed to the east of Kamchatka, when intersecting the 53°N latitude at 0959 UT, a high level of electron fluxes was detected in an energy range of 90.7–526.8 keV (Fig. 4b, upper curve). The growth in electron fluxes on that day began at latitudes close to 45°N. At a latitude of 53°N, it reached values of 10⁴–10⁵ electrons/s and did not decrease until the passage of the orbit point closest to the pole. In this energy range, the electron flux at a latitude of 53°N was in fact equal to the electron flux in the auroral zone. In the spectrum of erupted electrons that was obtained when intersecting the 53°N latitude, the maximal fluxes of particles were detected in an energy range of 90–140 keV. The values of the electron fluxes were on the order of 10³ electrons/cm²/s/sr.

Under the conditions of geomagnetic perturbations retained at that time, one can believe that close values of electron fluxes were also observed at that time over Kamchatka. This is verified by similarly large values of fluxes at a latitude of 53°N at the next orbit pass (after 1 h 38 min) at 1137 UT (Fig. 4c).

The presence of eruptions of soft electrons on March 28, 2008, over Kamchatka is verified by the simultaneous appearance of corpuscular-type sporadic *Es* layers detected by the Kamchatka AIS. At night, during lidar observations, sporadic *Es* layers of the corpuscular type with a critical frequency of 1.5–1.6 MHz were detected at heights of 135–150 km beginning from 0930 UT and up to the end of the measurements. In some cases, due to the absorption that was too high for nocturnal conditions, one could judge about the presence of *Es* exclusively by the shape of the trace of the *F2* layer. Figure 5 presents the ionograms obtained by the Kamchatka AIS on March 28, 2008, at the end of the lidar observations. According to the trace of an extraordinary wave, *foEs* can be determined in these ionograms as 1.55 MHz. A frequency

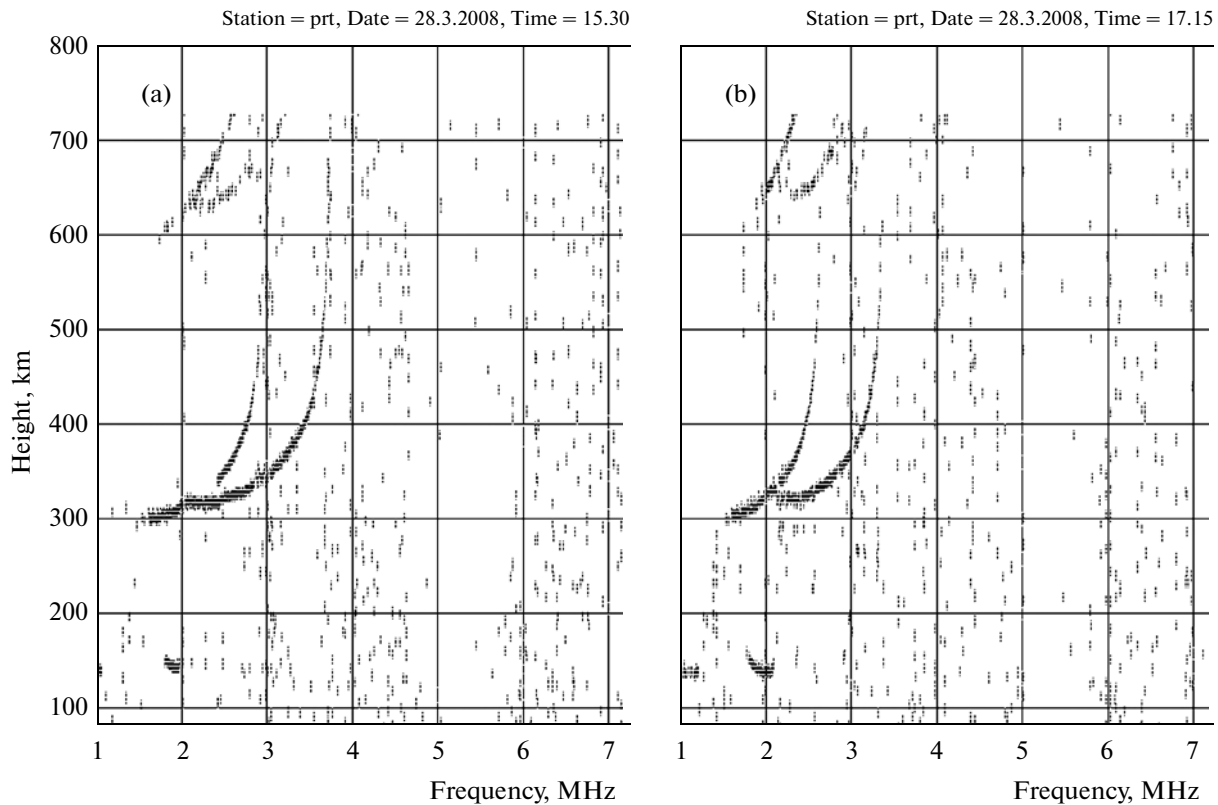


Fig. 5. Ionograms with Es layers of the corpuscular type obtained by the Kamchatka AIS on March 28, 2008.

of 1.55 MHz is in correspondence with an electron concentration of $3 \times 10^4 \text{ cm}^{-3}$.

Thus, the presence of eruptions of relativistic and soft electrons over Kamchatka at the time of the lidar observations on March 28, 2008, is verified by satellite and ionospheric data. At heights of ~ 150 km, according to the available ionospheric data, the rate of ionization by erupted electrons can be estimated as $1.36 \times 10^2 \text{ 1/cm}^3/\text{s}$. In a height range of 200–300 km, one can expect an ionization rate of about 20–90 $\text{1/cm}^3/\text{s}$. A justification of these estimates is presented in the Appendix.

4. DISCUSSION OF THE RESULTS

In correspondence with the lidar data for March 28, 2008, an increase in the total signal by ~ 100 photons during the period from 1300 to 1430 UT (Fig. 1b) is a pure accumulated signal. These are photons counted for each 15 min of observations (~ 9000 echo signals) during 90 min. With allowance for the FEM quantum efficiency equal to $\sim 30\%$, the actual number of incoming photons exceeds 100 by a factor of ~ 3 and is a significant value for the Poisson statistics. The absence of a correlation between the signal from the range 100–150 km and the decrease in the signal after a height of 300 km permits one to propose a hypothesis about the formation of a layer of scatterers with large

interaction cross-sections and with a maximum of the content in a range of 200–300 km.

The detected correlation between lidar signals and plasma density at ionospheric heights requires an explanation. One of the possible explanations is a hypothesis about the participation of highly excited, but not ionized, Rydberg atoms in the formation of lidar signals from these heights. In (Avakyan et al., 1997), Rydberg atoms were considered as a possible source of generation of proper microwaves and far IR radiation of the ionosphere. Below, we present the properties of Rydberg atoms properties taken from (Avakyan et al., 1997; Delone, 1998). The radius of the orbit of the Rydberg atom $r \sim n^2$, the geometric cross section $s \sim n^4$, the lifespan $\tau \sim n^3 - n^5$ depending on the values of the orbital quantum number, the polarizability $\alpha \sim n^7$, and the difference of energies between two excited levels $\Delta E \sim n^{-3}$. Here, n is the principal quantum number of the excited state. It is seen from the presented estimates that the properties of Rydberg atoms that define the cross-section of the interaction between an atom and radiation can vary by many orders of magnitude.

The light scattering cross-section for a single atom is determined by the formula $\sigma = 8|\alpha|^2\omega^4/(3\pi c^4)$, where α is the polarizability, ω is the frequency of the incident radiation, and c is the speed of light (*Encyclo-*

pedia of Physics, 1994). For $n = 10$, the scattering cross-section decreases by 14 orders of magnitude because it is proportional to the square of the polarizability. The mean cross-section of molecular scattering in the visible range in conversion to one particle is $\sim 10^{-27}$ cm²/sr. It follows from these estimates that, for $n = 10$, cross-section σ is $\sim 10^{-13}$ cm². In (Avakyan and Voronin, 2006), the geometric cross-section of such atoms was estimated as $\sigma \sim 10^{-12}$ cm² for $n = 10$ and $\sigma \sim 10^{-11}$ cm² for $n = 20$. The characteristic transverse size of the scattering cross-section of such atoms and molecules becomes comparable with a wavelength of 532 nm used in observations.

In (Tarr et al., 1982), the formation of long-lived metastable states of highly excited Rydberg atoms was considered in an experiment with an electron impact. Atoms were detected by ionization in an electric field. The characteristic lifespan of excited atoms in this experiment is on the order of ~ 10 μ s. It was noted in that work that processes, such as predissociation and autoionization, become impossible at large values of the orbital angular momentum. High values of the orbital angular momentum, in turn, are not formed during photoabsorption due to the selection rules but can be very well excited by an electron impact at a small energy level of a particle. For electrons with energies in a range from 15 to 60 eV, the cross-sections of the Rydberg excitation process exceed the cross-sections of all other ionization and excitation processes for the main components of the upper atmosphere: N₂, O₂, and O (Banks and Kockarts, 1973).

In (Avakyan and Voronin, 2006), data on the lifespan of Rydberg atoms were presented. For a height of 100 km, it can be estimated by the formula $\tau \sim n^4 \times 10^{-9}$ s. In (Avakyan, 2006), the calculation results of the increase in the time between collisions of Rydberg atoms with neutrals with an increase in height from 100 to 250 km were presented. With a decrease in the density of the atmosphere, this time increases by 4–5 orders of magnitude at a height of 250 km. In the examples presented in that work, for states with principal quantum number n equal to 10 and 20 and for cross-sections of 10^{-12} cm² and 10^{-13} cm² at a height of 250 km, this time varies from values less than 0.01 ($s = 10^{-12}$ cm²) to ~ 0.5 s ($s = 10^{-13}$ cm²). Since collisions with neutrals are the main process determining the death of excited atoms, the lifespan of such states at heights of 250 km must be on the same order of magnitude. In a classical textbook on nuclear physics (Shpol'skii, 1984), it is noted that the lifespan of metastable states can reach 10^{-3} –1 s and examples of excited states of oxygen atoms with a lifespan of 42 s were presented: these are the ¹D₂, ¹D (100 s), and ¹S (0.5 s) states.

In (Avakyan and Voronin, 2006), the calculation results for the total rate of Rydberg state excitation for oxygen atoms and nitrogen and oxygen molecules for the nocturnal auroral ionosphere were presented. At a

height of 105 km, the total rate of formation of excited atoms is $\sim 10^4$ 1/cm³/s. For partial states, this rate is on the order of 10^2 1/cm³/s. At a height of 250 km, the excitation rates for specific Rydberg states are from 1 to 5 1/cm³/s. According to these estimates, the content of such atoms, which is equal to the rate of formation multiplied by the lifespan, has a maximum in the region of 250 km or higher.

Simple estimates show formation rates that are sufficient to obtain the observed signal. The area of the receiving mirror of the telescope is 0.28 m². Under the assumption of isotropic scattering, the ratio of the mirror area to the total surface of scattering from a height of 250 km is $\sim 5.7 \times 10^{-12}$. The divergence of the laser beam with a collimator is ~ 0.06 mrad. At a height of 250 km, the spot diameter is ~ 15 m. The illuminated volume in the layer from 200 to 300 km is $\sim 5.6 \times 10^{12}$ cm³. If one act of scattering occurs every second in every cubic centimeter of the volume, then ~ 1 photon/s falls on the mirror. During the observations of March 28, 2008, the detected rate of incoming photons was lower by an order of magnitude. With allowance for the quantum efficiency of the FEM, a scattering rate of 0.3 photons/cm³/s is sufficient to explain the observed signal.

The large geometric cross-sections of Rydberg atoms (10^{-12} cm² for $n = 10$) (Avakyan and Voronin, 2006) ensure a high probability of their interaction with the laser pulse radiation ($\sim 3.5 \times 10^{14}$ photons/cm²/s at a height of 250 km). When the laser frequency is 10 Hz, all formed atoms, the lifespan of which is larger than 0.1 s, interact with radiation with a large probability. Ionization by electrons always takes place in the ionosphere, and, at the end of the process of energy spending for individual ionization acts, all newly formed electrons finally become less energetic with larger excitation cross-sections of the Rydberg states of atoms and molecules, including metastable states.

The presented estimates of the ionization rate on March 28, 2008, which are equal to 20–90 1/cm³/s in a height range of 200–300 km, give grounds to suppose that these electrons can ensure the formation of three atoms during 10 s with necessary sizes and a lifespan sufficient for their interaction with a photon with a wavelength of 532 nm. The interaction between such atoms and laser radiation can cause its scattering if the photon energy at a wavelength of 532 nm which is equal to 2.4 eV is not sufficient for the ionization of an excited atom.

There is a necessity in more rigorous estimates, including calculations of ionization functions and estimates of excitation rates for Rydberg states, attenuation of the radiation intensity in the atmosphere, and allowance for the scattering phase function. There is also a necessity in additional studies with the aim to determine the specific mechanism of scattering. This must be atoms or molecules in states ensuring a suffi-

cient size and lifespan to obtain the observed signal. This may not be states with too large a value of the principal quantum number; the difference between the ionization potential and the energy of the excited state must exceed the photon energy equal to 2.4 eV at a wavelength of 532 nm. Both conditions are satisfied by excited atoms and molecules with a principal quantum number close to 10.

5. CONCLUSIONS

All of the above-listed is the subject of a separate study; however, even now one can conclude that lidar signals from ionospheric heights correspond to the obtained estimates in the order of magnitude. As for the correlation between lidar signals and plasma density at the maximum of the *F2* layer that was repeatedly observed in 2008 at Kamchatka during geomagnetic perturbations, it can also be explained by the scattering process on excited atoms.

APPENDIX A:

Estimating the Ionization Rate by Erupted Electrons

The sporadic *Es* layers presented in Fig. 5 appeared during lidar observations at heights of ~150 km. The ionization rate by electrons in this height region can be estimated from the following reasoning. Assuming that the condition of photochemical equilibrium is satisfied below heights of 150 km and that the fraction of O^+ ions at 150 km is still small as compared to the content of molecular ions, one can ignore the presence of O^+ ions for estimates on the order of magnitude and write the condition of photochemical equilibrium in the form

$$N_e = ((q(O_2) + q(N_2))/\alpha)^{1/2},$$

$$\text{or } q = q(O_2) + q(N_2) = \alpha N_e^2,$$

where $q(O_2)$ and $q(N_2)$ are the ionization rates of O_2 and N_2 , respectively; α is the coefficient of dissociation recombination, which, for approximate estimates for middle and low latitudes, can be taken equal to (Deminov, 2008)

$$\alpha = (\alpha_1 + \alpha_2)/2, \quad \alpha_1 = (3.5 \pm 0.5) \times 10^{-7} (300/T_e)^{0.69},$$

$$\alpha_2 = 1.95 \times 10^{-7} (300/T_e)^{0.70};$$

$N_e = 3 \times 10^4$ 1/cm³ is the electron density measured by the AIS; and T_e is the temperature of electrons.

For nocturnal conditions and a height of 150 km, one can assume that $T_e = T_i = T_n$. Here, T_e , T_i , and T_n are the temperatures of electrons, ions, and neutral component of plasma, respectively. According to the data of the NRLMSISE-00 model (Picone et al., 2002), at a height of 150 km for the latitude and longitude of Kamchatka, the temperature $T_n \sim 700$ K at night in March.

Assuming that $T_e = T_n$, we obtain $\alpha_1 = 1.95 \times 10^{-7}$; $\alpha_2 = 1.08 \times 10^{-7}$, and $\alpha = 1.51 \times 10^{-7}$ (cm³/s).

Then, for the ionization rate at a height of 150 km, we obtain $q = 1.36 \times 10^2$ 1/cm³/s.

In (Deminov and Khagai, 1980), height profiles of the ionization rate normalized by the integral flux of erupted electrons in a height range of 80–300 km are presented. For the Maxwell spectrum, the maximum of ionization produced by electrons at a height of 150 km corresponds to an electron flux with the characteristic energy $E_0 \sim 0.5$ keV.

Calculations by the formula for the ionization rate by electrons presented in (Deminov, 2008) show that, for $E_0 = 0.5$ keV, the ionization rate decreases by a factor of ~1.5 at a height of 200 km; by a factor of ~3 at a height of 200 km; and by a factor of 7.5 at a height of 300 km. In a height range of 200–300 km, one can expect the ionization rate to be about 20–90 1/cm³/s.

APPENDIX B:

Estimating the Statistical Significance of the Correlation Coefficient

Let us denote the total signals from heights of 150–200 and 200–300 km as *X* and *Y*, respectively. The initial data are as follows:

X, 153.9, 159.46, 64.31, 98.02, 93.99, 116.95, 91.18, 120.92, 134.81, 75.34, 71.71, 40.02, 95.09, 108.13, 171.24, 118.93, 184.02, 167.09, 163.29, 164.12, 156.86, 165.62, 191.71, 131.88, 160.02, 142.5, 140.71, 15.75.

Y, 223.92, 189.28, 139.09, 140.01, 109.26, 70.84, 121.24, 118.55, 152.53, 85.04, 141.23, 46, 164.57, 184.13, 174.28, 211.5, 222, 192.6, 198.99, 215.08, 228.77, 250.14, 258.36, 201.5, 200.44, 182.79, 180.92, 100.6.

The dimension of data $n = 28$. The mathematical expectation and variance for *X* and *Y* are as follows:

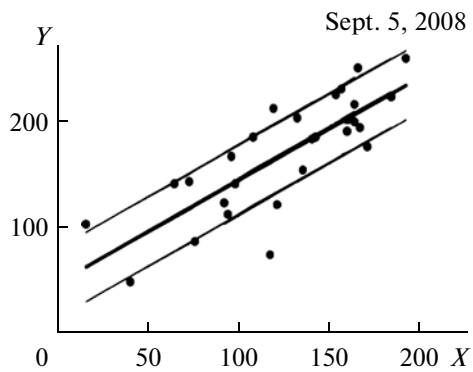
$$\begin{aligned} MX &= 124.9, & DX &= 1989.8, \\ MY &= 167.99, & DY &= 2964.94. \end{aligned}$$

The correlation coefficient $r_{xy} = 0.8$.

The tabulated value of Student's test at a significance level of 0.10 and $n = 28$ $T_t(0.10, n - 2) \approx 1.706$. The value calculated by the available data is $T_n = r_{xy} ((n - 2)/(1 - r_{xy}^2))^{1/2} \approx 6.85$. Since $|T_n| > T_t$, one can conclude that the r_{xy} value is statistically significant and the 90% confidence interval for r_{xy} is

$$\begin{aligned} (r_{xy} - T_t(1 - r_{xy}^2)/n^{1/2}), \\ (r_{xy} + T_t(1 - r_{xy}^2)/n^{1/2}) = (0.68 - 0.92). \end{aligned}$$

The regression equation for *Y* on *X* has the form $y = 0.98x + 45.98$.



1 **Fig. 6.** Regression line for the lidar data obtained on September 5, 2008.

Figure 6 presents the values of the X and Y arrays and a regression line for Y on X with an error of one standard deviation defined as $\sigma = (\sum(y - Y_i)^2 / (n - 2))^{0.5}$.

ACKNOWLEDGMENTS

This work was supported by the Far Eastern Branch, Russian Academy of Sciences (projects nos. 12-I-P10-01 and 12-I-OFN-16); Russian Foundation for Basic Research (project no. 10-05-00907-a); and by the Siberian Branch, Russian Academy of Sciences (integration project no. 106).

REFERENCES

Avakyan, S.V., Serova, A.E., and Voronin, N.A., Role of Rydberg Atoms and Molecules in the Upper Atmo-

sphere, *Geomagn. Aeron.*, 1997, vol. 37, no. 3, pp. 99–105.

Avakyan, S.V., Collisions of Rydberg-Excited Neutrals in the Ionosphere and Microwave Radiation, *J. Opt. Technol.*, 2006, vol. 73, no. 4, pp. 302–303.

Avakyan, S.V. and Voronin, N.A., Condensation Process in the Low Atmosphere and Microwave Radiation of the Sun and Ionosphere, *Proc. 6th Intern. Conf. on Problems of Geocosmos*, St. Petersburg, 2006, pp.24–28.

Banks, P.M. and Kockarts, G., *Aeronomy*, New York: Academic Press, 1973.

Delone, N.B., Rydberg Atoms, *Sorosovskii obrazovatel'nyi zhurnal*, 1998, no. 4b, pp. 64–70.

Deminov, M.G., Earth's Ionosphere, in *Plasmennaya geliofizika* (Plasma Heliogeophysics), Zelenyi, L.M. and Veselovskii, I.S., Eds., Moscow: Fizmatlit, 2008, vol. 2, pp. 92–163.

Deminov, M.G. and Khagai, V.V., Analytical Approximation of the Ionization Rate by Auroral Electrons, *Geomagn. Aeron.*, 1980, vol. 20, no. 1, pp. 145–147.

Entsiklopediya fiziki (Encyclopedia of Physics), Prokhorov, A.M., Ed., Moscow: Bol'shaya Rossiiskaya Entsiklopediya, 1994, vol. 4, pp. 277–282.

Picone, J.M., Hedin, A.E., Drob, D.P., and Aikin, A.C., NRLMSISE-00 Empirical Model of the Atmosphere: Statistical Comparisons and Scientific Issues, *J. Geophys. Res.*, 2002, vol. 107, no. A12, pp. 1468–1483.

Shpol'skii, E.V., *Atomnaya fizika* (Nuclear Physics), Moscow: Nauka, 1984.

Tarr, S.M., Schiavone, J.A., and Freund, R.S., Long-Lived High-Rydberg Molecules Formed by Electron Impact: H_2 , D_2 , N_2 and CO , *J. Chem. Phys.*, 1981, no. 5, pp. 2869–2878.

SPELL: 1. lidar, 2. singularities, 3. polarizability, 4. predissociation